SUPPLEMENTAL TEXT AND FIGURES

Figure S1: Schematic for quantification of intercellular (cell-free) spaces within the LR DM from HH17-21 using ImageJ (related to Figure 1).
A (Left panel) Cartoon model of a transverse section of HH21 midgut-DM showing condensed left (orange) and expanded right (blue) mesenchyme. (Middle panel) H&E of HH19 midgut section. Orange and blue boxes indicate regions selected for analysis of cell-free spaces. (Right panel) The selected regions were copied to a new window in ImageJ (step 1) and cell-free spaces were identified using the ImageJ Thresholding Tool with a dark background option (step 2). These were then segmented into smaller parts using the Watershed Algorithm Tool and the sum total of their areas were estimated with the Particle Analyzer Tool. **B** Cartoon of the right lateral view of an embryo with the midgut region defined. The midgut has been segregated into five zones, Z1-Z5, where Z1 has been defined as the caudal midgut, Z2-Z3 the mid-caudal midgut, and Z4-Z5 as the central midgut. Examples of H&E images of the caudal, mid-caudal, and central midgut regions are shown in the right panel. Graphs demonstrate significant variation in expansion of the right DM across the different defined midgut regions at HH18-21 where the mid-caudal and central regions show more expansion than the caudal region (orange is left DM, blue is right DM, p values are indicated within the graphs; error bars represent mean ± SEM for n = 5 chicken embryos per developmental stage). Scale bars: **A, B** (50 μm).

Figure S2: Vascular exclusion on the right is coincident with initiation of the leftward gut tilt (related to Figures 3 and 4).
Endothelial cells of the right-sided DV cords (HH17) are progressively excluded from the right as DM expansion proceeds starting at HH18, resulting in strictly left-sided DV cords at HH20. This was observed via RNA ISH for *VE-cadherin* in the chicken (n =5 embryos) **A** and Tie1-H2B-YFP quail embryos (n = 5 embryos) **B**. **C** Model of the spatiotemporally coordinated DM expansion, formation of the leftward gut tilt, and vascular exclusion of the DV cords. Scale bars: **A, B** (100 μm).

Figure S3: Relationship between Tsg6-HA pathway and *Pitx2* expression (related to Figures 2, 4, and 8).
A (Top panel) *Pitx2* RNA ISH on HA depleted embryos on the right confirms left-sided *Pitx2* expression in the DM is not affected despite loss of the leftward gut tilt (p = 0.99 for DMSO vs MU-Xyl, n = 5/5 for DMSO, n = 8/8 for MU-Xyl). (Bottom panel) The expression of *Gpc3*, a downstream Pitx2 target and effector of the non-canonical Wnt signaling is also not altered in these embryos as demonstrated by the left-restricted DM expression of *Gpc3* (RNA ISH to *Gpc3*) (p = 0.99 for DMSO vs MU-Xyl, n= 5/5 for DMSO, n = 3/3 embryos for MU-Xyl). **B** *Pitx2* RNA ISH on chicken embryos with electroporated *Tsg6* confirms left-sided *Pitx2* expression in the DM is not affected (p = 0.8592 for WT vs pCAGEN-Tsg6, n = 5/5 embryos for both). Scale bars: **A** (left panel, 100 μm; right panel, 50 μm); **B** (50 μm).

Figure S4: Expression profile of *Tsg6* in the chicken DM (related to Figure 4)
RNA ISH for *Tsg6* in the chicken DM demonstrates that right-sided expression of *Tsg6* coincides with DM expansion (n = 10 embryos per stage). Scale bars: 100 μm.

Figure S5: Additional Tsg6-specific morpholinos (related to Figure 4)
A Cx40 RNA ISH of whole embryos demonstrates normal 1° and 2° LA development in control SC-MO. In Tsg6-sMO electroporated embryos (**B**), 1°LA is lost and anomalous 2°LA-like vessel forms (green arrows). Red arrowheads depict 1°LA, green arrows depict 2°LA. ($p = 0.005$ for SC-MO vs Tsg6-sMO, n = 0/9 for SC-MO, n = 4/5 for Tsg6-sMO) **C** *Pitx2* RNA ISH on Tsg6-tMO right-side electroporated embryos confirms left-sided *Pitx2* expression in the DM is not affected despite loss of the leftward gut tilt ($p = 0.99$ for WT vs Tsg6-tMO, n = 8/8 for WT, n = 5/5 for Tsg6-tMO).
Scale bars: **A, B** (200 μm); **C** (100 μm).

Figure S6: *Tsg6* is sufficient to drive DM vascular exclusion but not ECM expansion on the left (related to Figures 4 and 5).
A (Top panel) Anti-angiogenic effect of *Tsg6* misexpression on the left is dosage dependent. Complete loss of DM vasculature is seen in embryos strongly electroporated with pCAGEN-*Tsg6* on the left side ($p = 0.0005$ for WT vs pCAGEN-*Tsg6*, n = 0/15 for WT, n = 11/19 for pCAGEN-*Tsg6* embryos). (Bottom panel) Weakly electroporated embryos show only partial loss of the 1°LA (n=8/19). **B** (Top panel) pCAGEN-*Tsg6* is not sufficient to induce expansion of the DM mesenchyme when electroporated on the left (n = 15 embryos) **C** embryos electroporated with catalytically inactive Tsg6 (S28A) mutant on the right) showing Tsg6 is necessary for expansion (n = 5 embryos).
Scale bars: **A** (100 μm); **B, C** (50 μm).

Figure S7: Molecular characterization of Tsg6-HA pathway in the mouse and rat DM (related to Figure 7).
(Top panel) LR asymmetric molecular and cellular differences are conserved in mice and rat DM at the cranial midgut region (mice n = 5 embryos, rat n = 8 embryos). While *Pitx2* is restricted to the left DM, HA staining and expression of I-α-I and Tsg6 proteins are restricted to the right DM. **Bottom:** Cartoon showing mechanism of heavy chain (HC) modification of HA by transfer of heavy chains from I-α-I, catalyzed by Tsg6, modified and adapted from (Lauer et al., 2013b).
Scale bars: Mouse 50μm; Rat 30μm

Figure S8: *Tgs6* -/- mice are predisposed to midgut volvulus (related to Figure 7).
A The distance (in microns) between the duodenojejunal junction (DJJ) and ileocecal junction (ICJ) (red double-headed arrow) and of the abdominal length (green double-headed arrow) was measured in *Tsg6* +/+ and *Tsg6* -/- E18.5 embryos (top panel). The ratio of the two values were plotted (bottom panel) and compared against the threshold value for defining a narrow mesenteric stalk (black dotted line) reflective of increased predisposition to volvulus ($p = 0.0172$ for WT vs *Tsg6* -/-, n = 0/7 for WT, n = 4/5 for *Tsg6* -/-). The *Tsg6* -/- mutant embryo marked with red asterisk (n = 1/5) had normal looping morphology. **B** Analysis of gut looping in E13.5 mouse embryos shows defects in orientation of the jejunal and ileal loops in *Tsg6* -/- embryos ($p = 0.035$ for WT vs *Tsg6* -/-, n = 0/8 for WT, n = 3/5 for *Tsg6* -/-)
Scale bars: **A** (1000 μm); **B** (500 μm).

Table 1: Unexpected Mendelian genetics for *Tsg6* mouse strain (related to Figure 7).
Table representing Mendelian analysis of *Tsg6*-null mice demonstrates deviation from the expected Mendelian inheritance ratios. Female *Tsg6* -/- mice are infertile, thus a *Tsg6* +/- female

is typically bred with a *Tsg6* -/- male. However, we find a reduction in recovery of *Tsg6* -/- mutant embryos at birth (30% [26/85 *Tsg6* -/- mouse embryos] versus the expected 50% [42.5/85]), pointing to partial embryonic lethality phenotypes associated with loss of *Tsg6*.

A Quantification of intercellular spaces (cell-free) using ImageJ

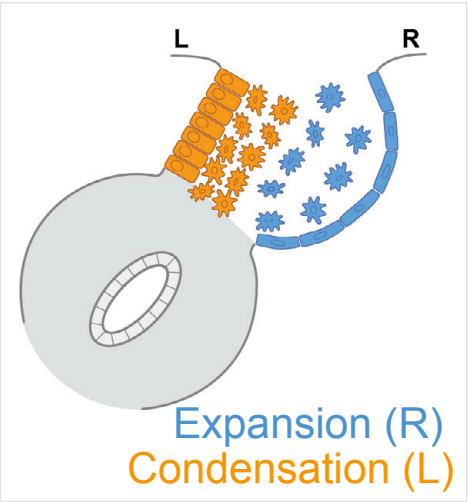

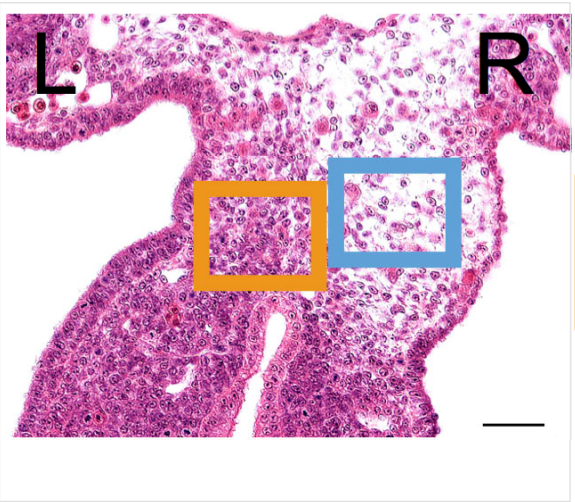

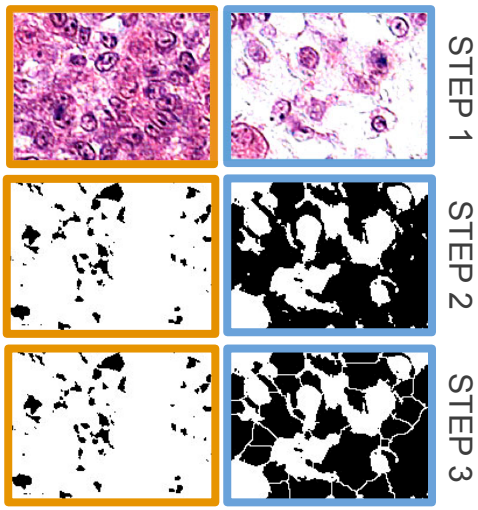

B Expansion of the right DM varies across the A-P axis

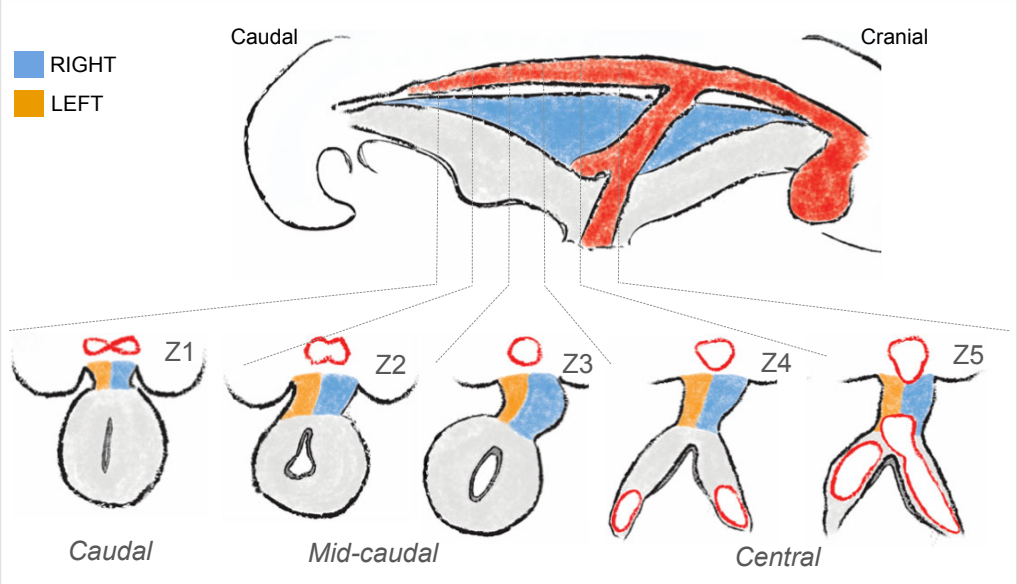

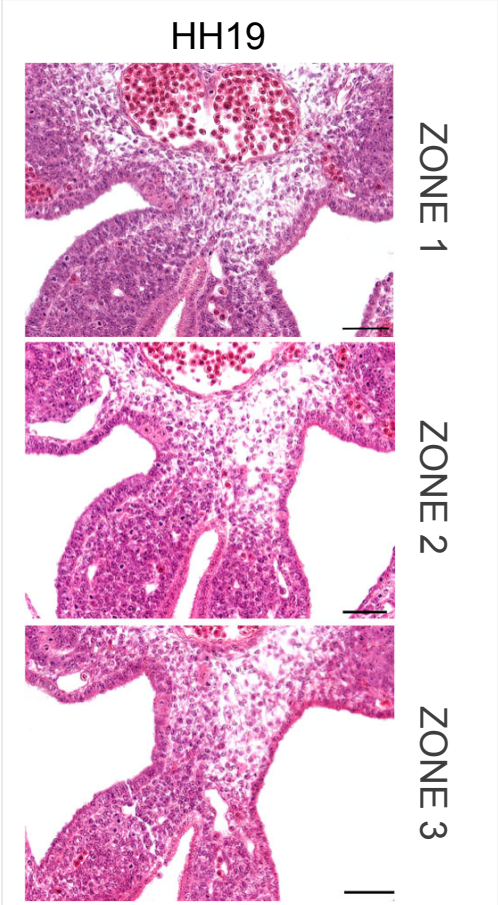

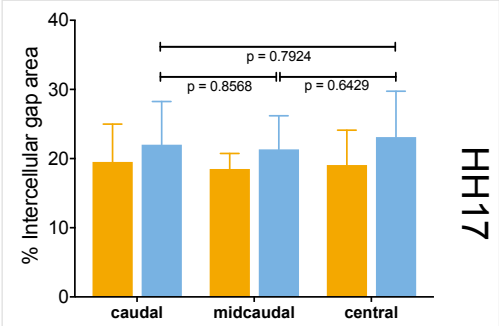

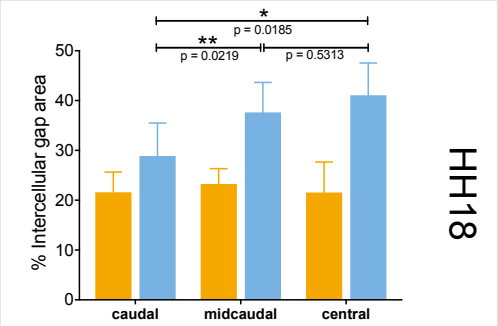

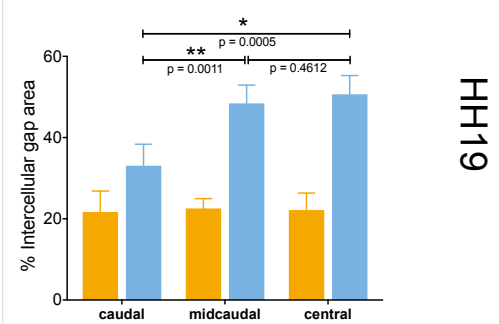

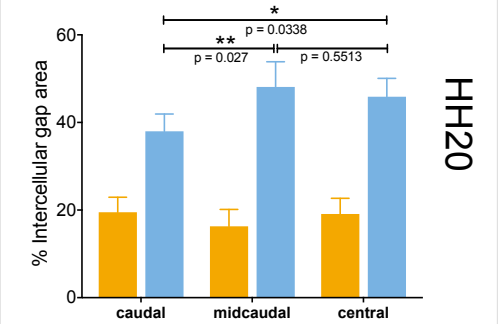

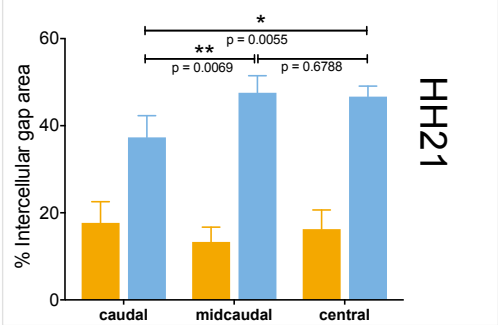

A The right DM becomes avascular during the formation of the leftward tilt *(VE-cadherin)*

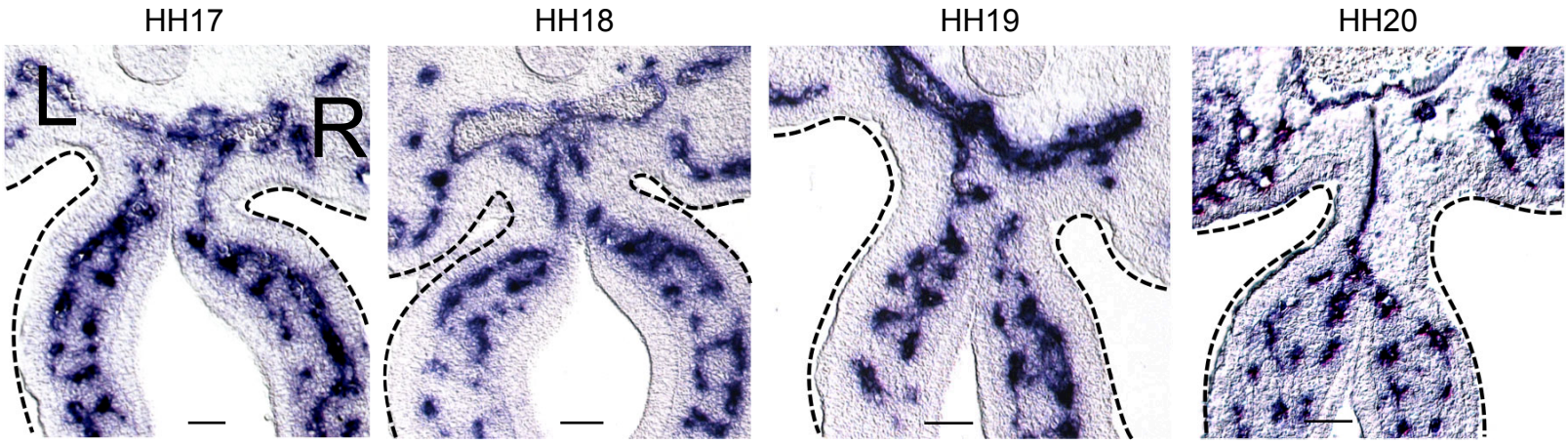

B The right DM becomes avascular during the formation of the leftward tilt (Tie1-YFP)

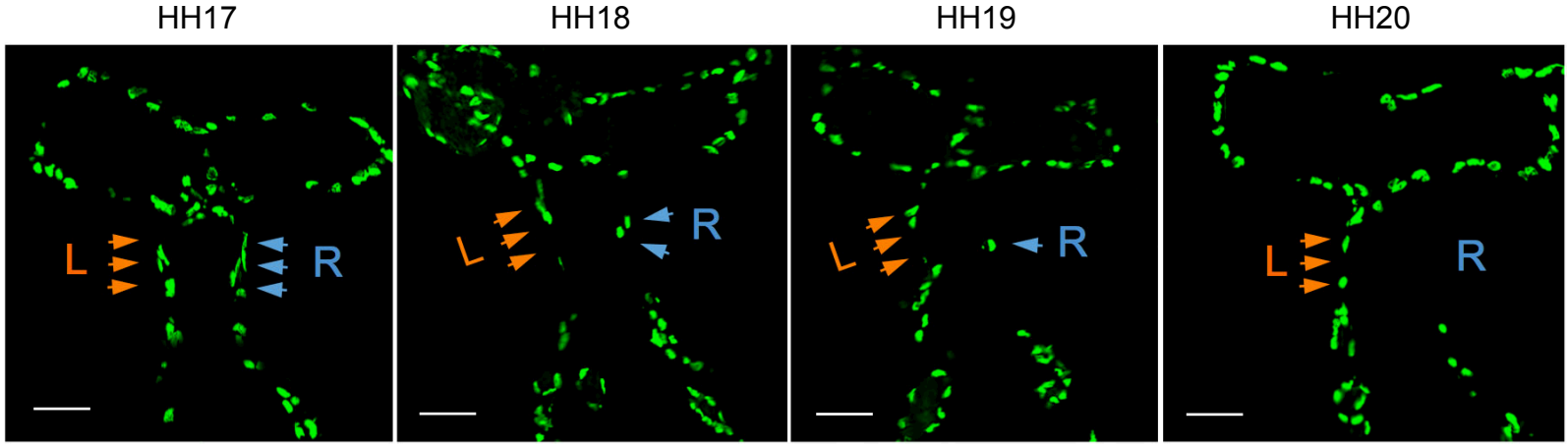

C Vascular exclusion coincides with DM expansion on the right

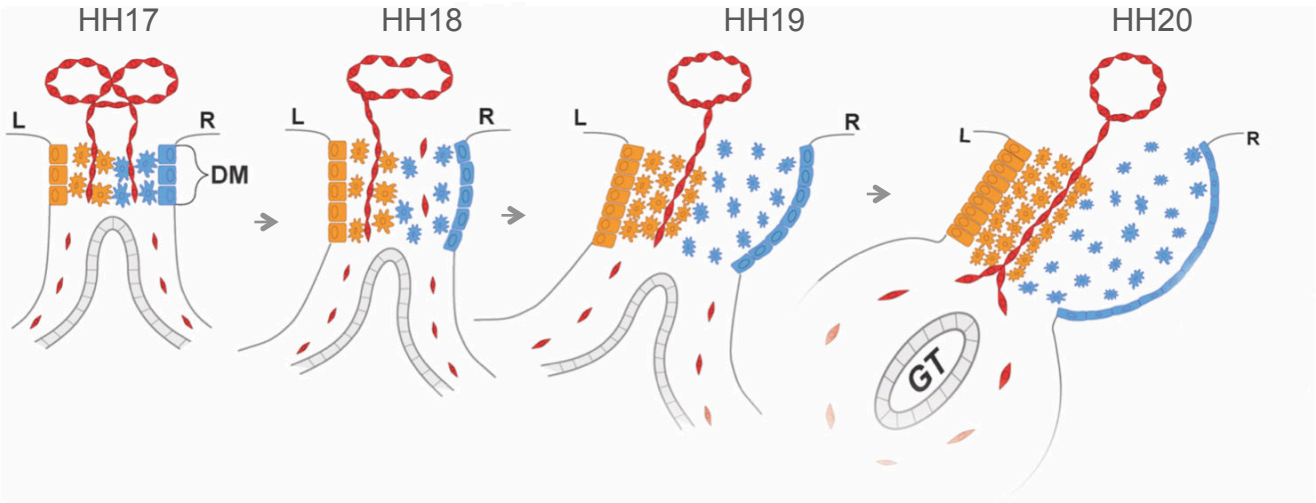

A HA depletion on the right prevents gut tilting without affecting *Pitx2* expression

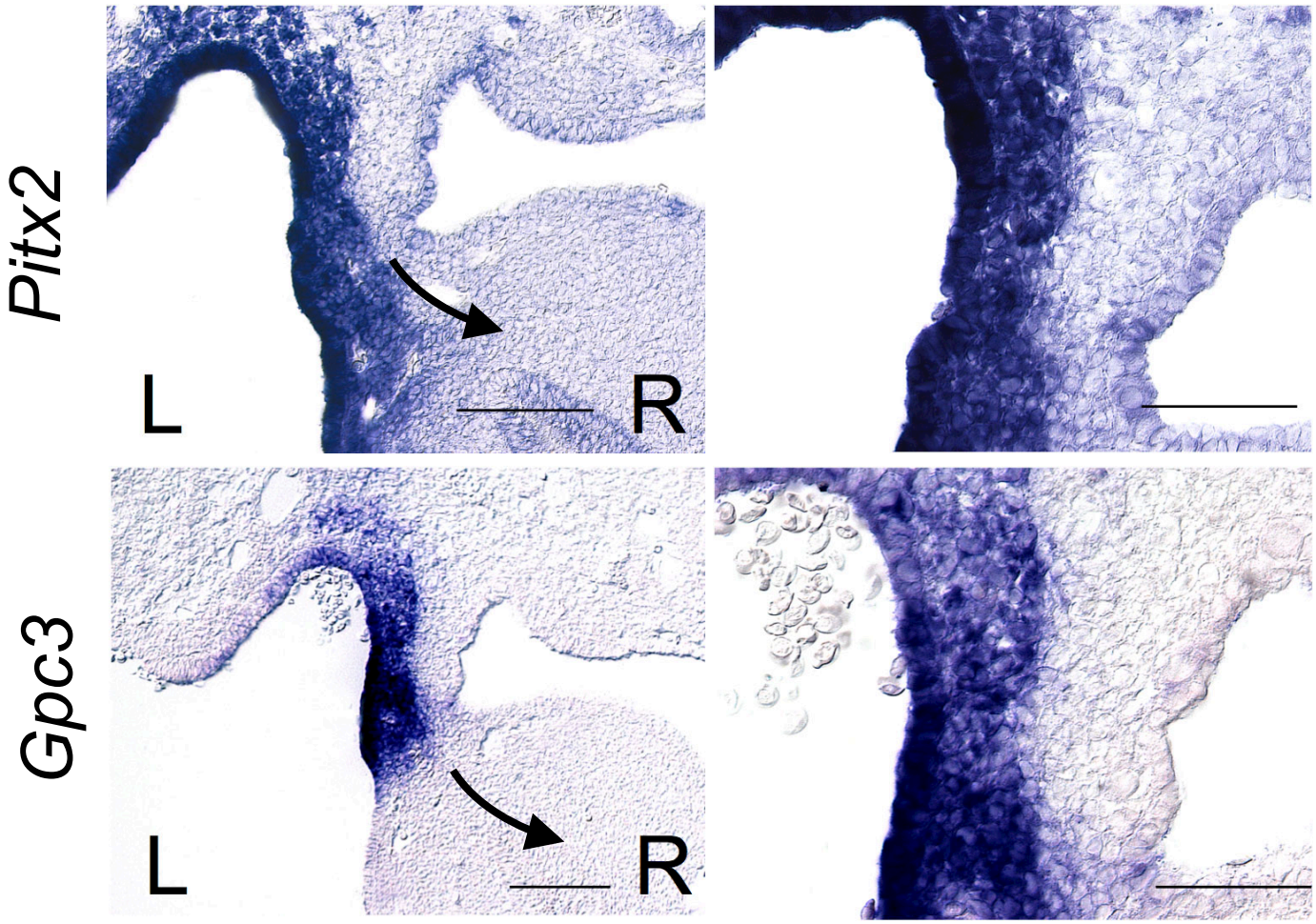

R: MU-Xyl

B Electroporating Tsg6 on the left does not affect *Pitx2* expression

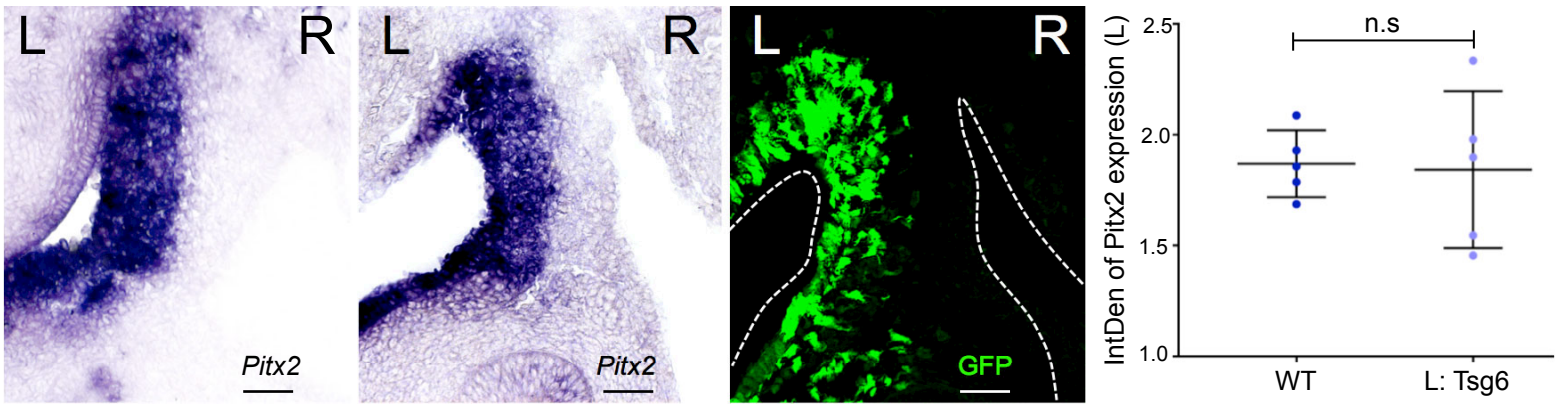

Tsg6 expression is right sided and initiates with ECM expansion and HA production

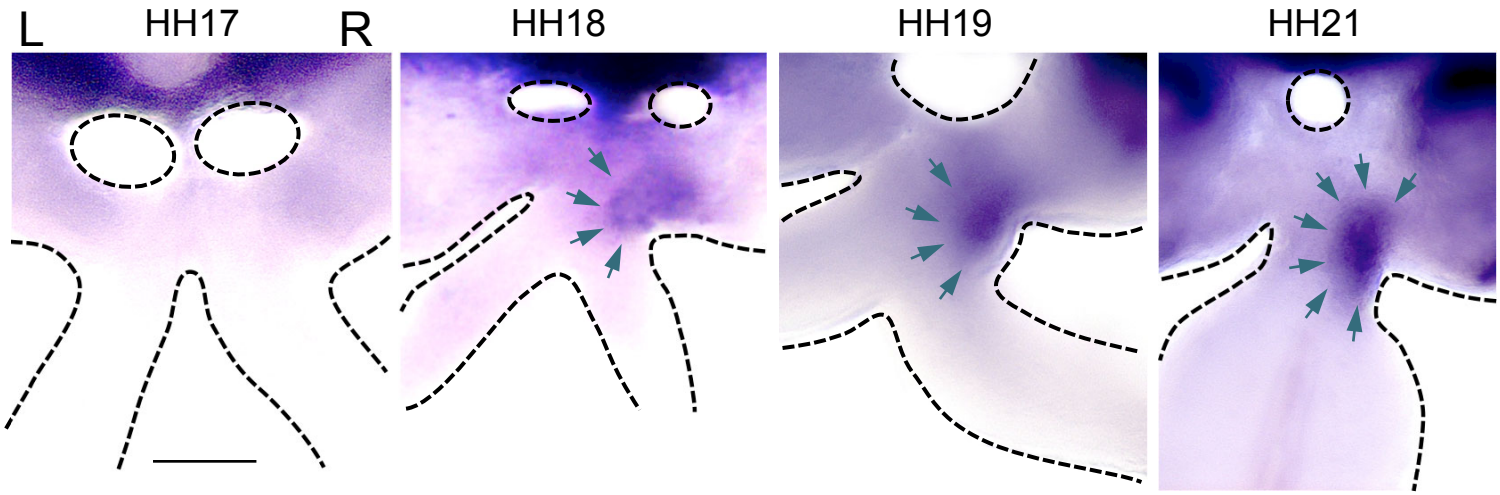

A R: Tsg6-tMO (HH25)

B Additional controls R: Tsg6-sMO (HH25)

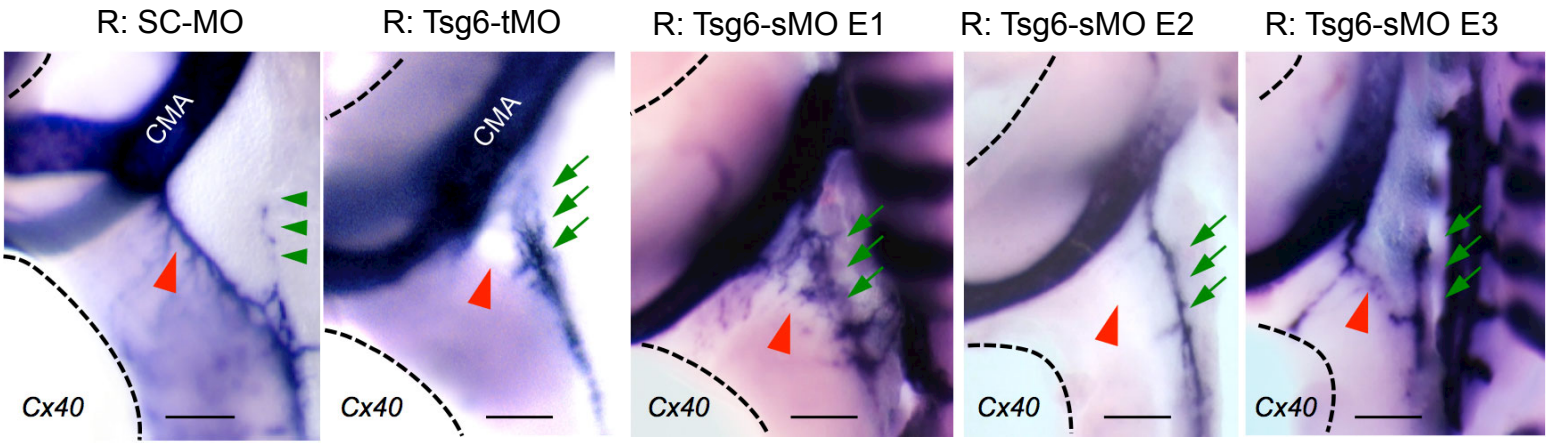

C Loss of *Tsg6* in the right DM has no effect on the left sided regulatory pathway

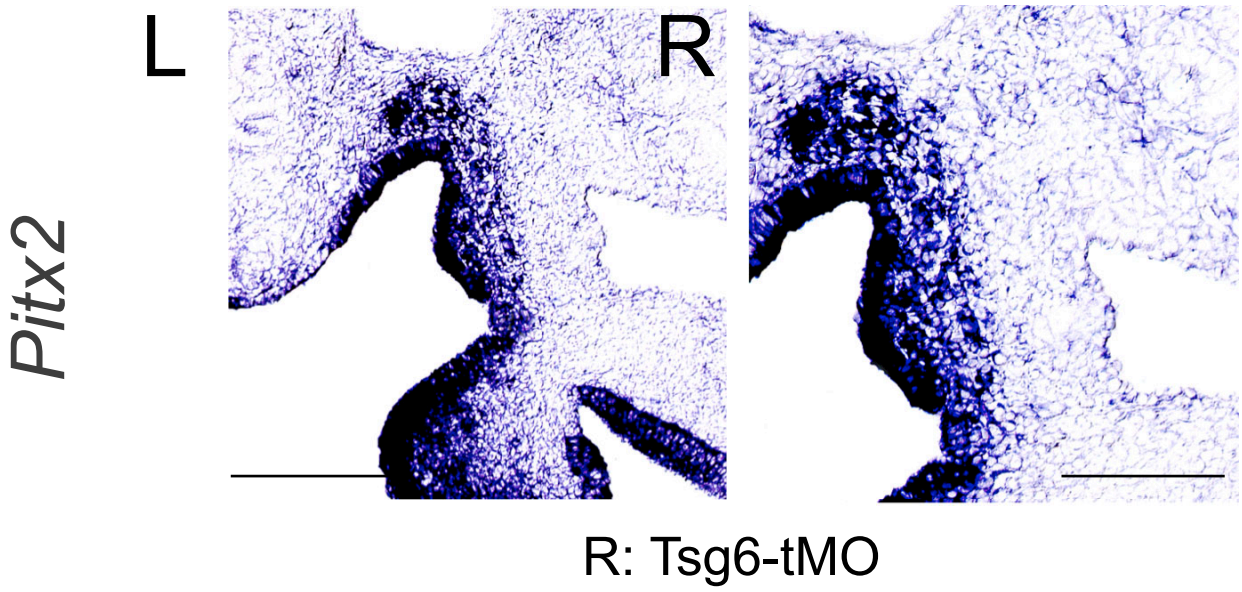

A The anti-angiogenic effect of Tsg6 is dosage dependent

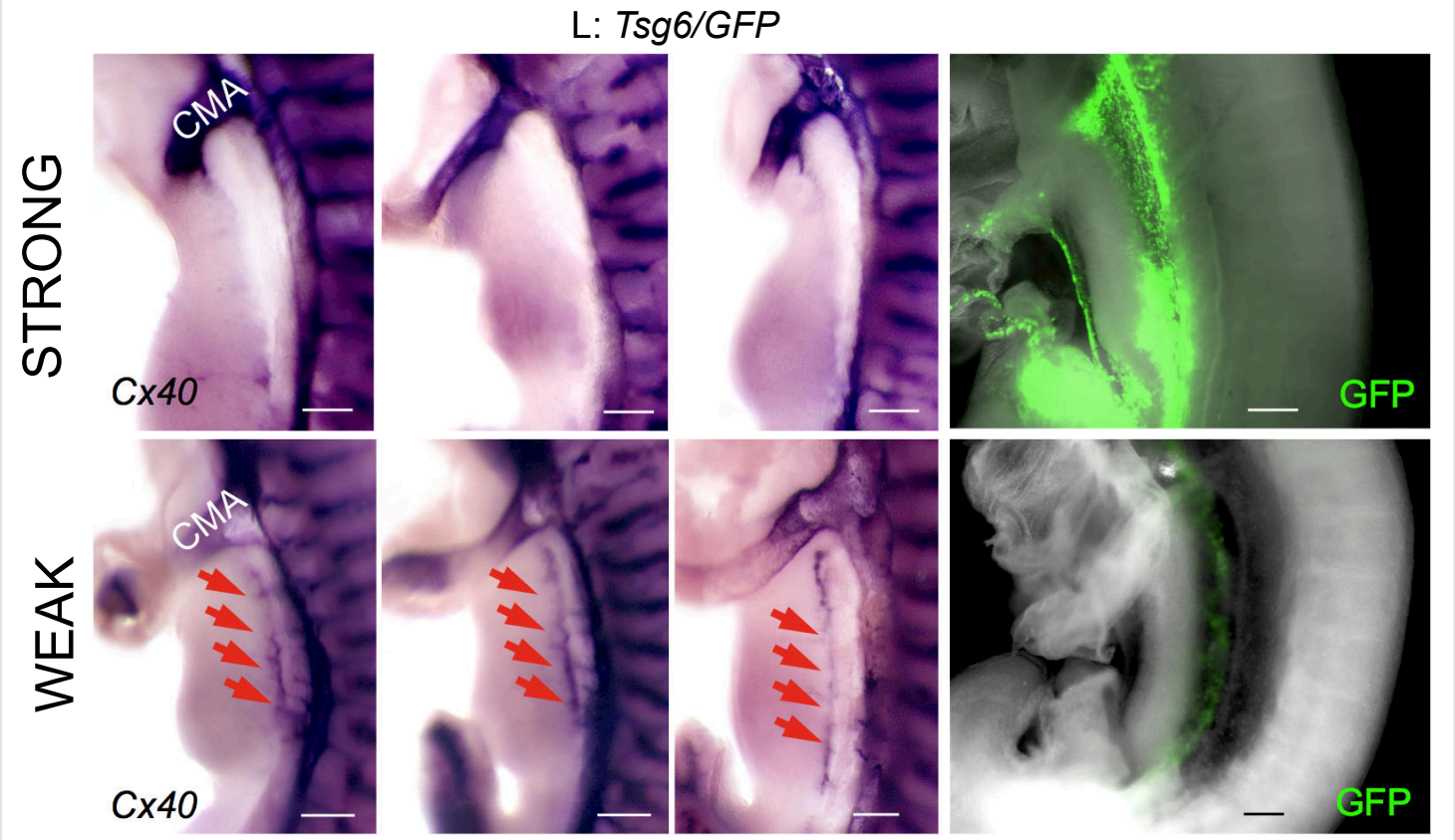

B Electroporating WT Tsg6 on the left is not sufficient to cause DM expansion

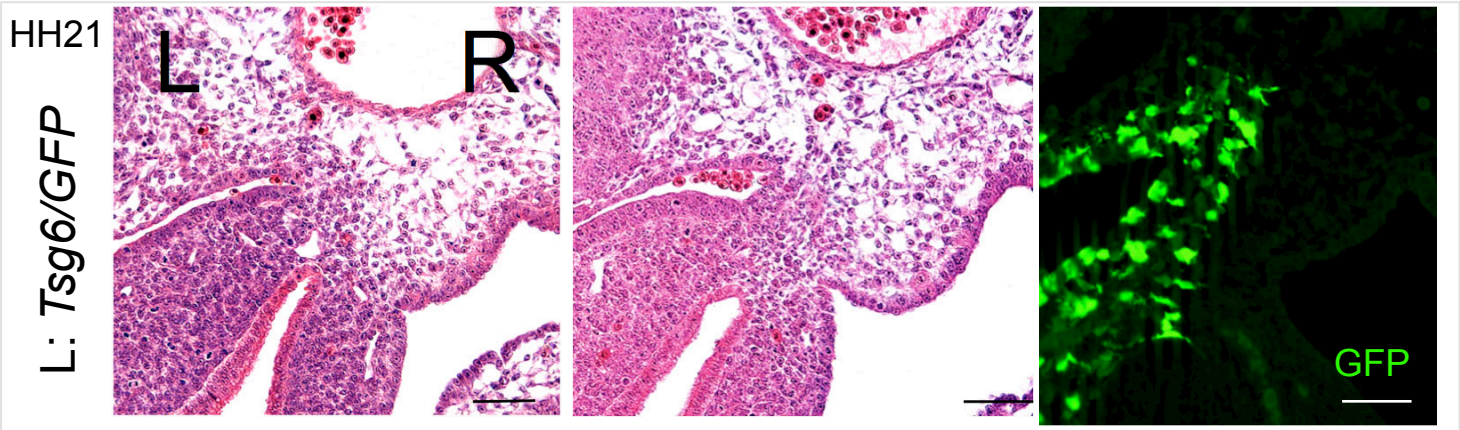

C Electroporating Tsg6-S28A on the right results in the loss of DM expansion

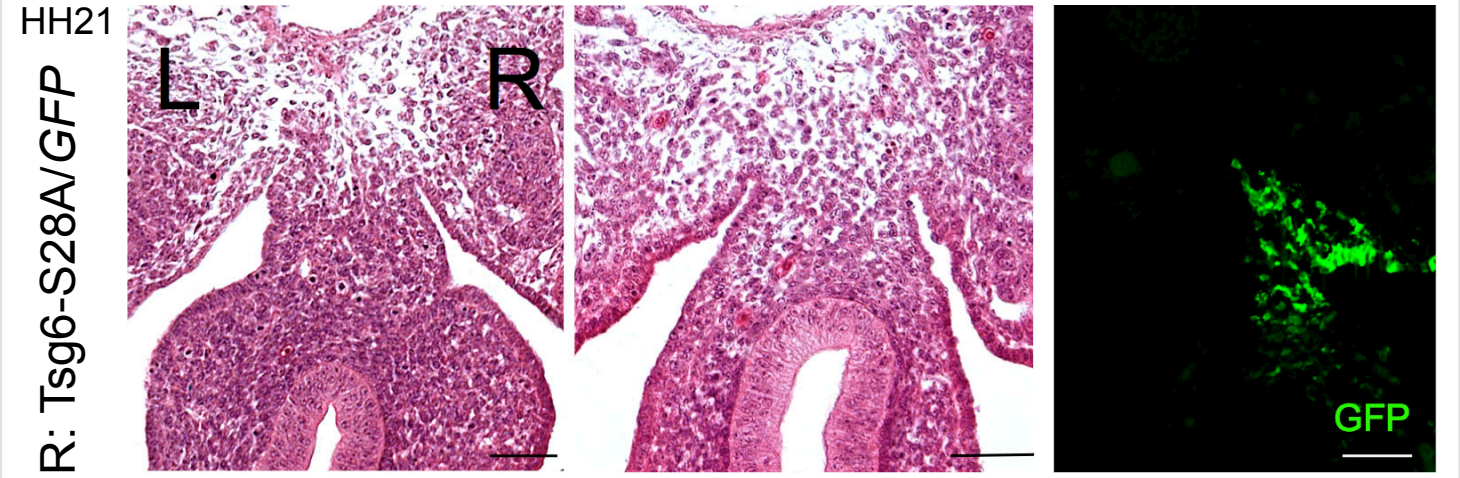

Molecular asymmetries of HC-HA components are conserved in the mouse DM

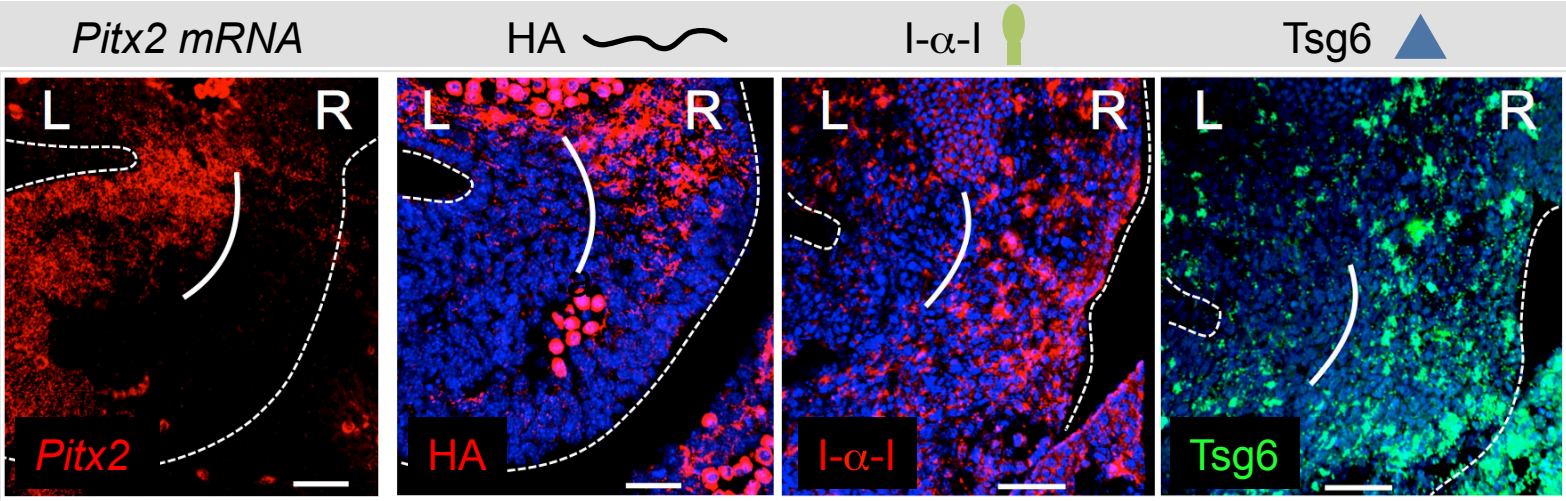

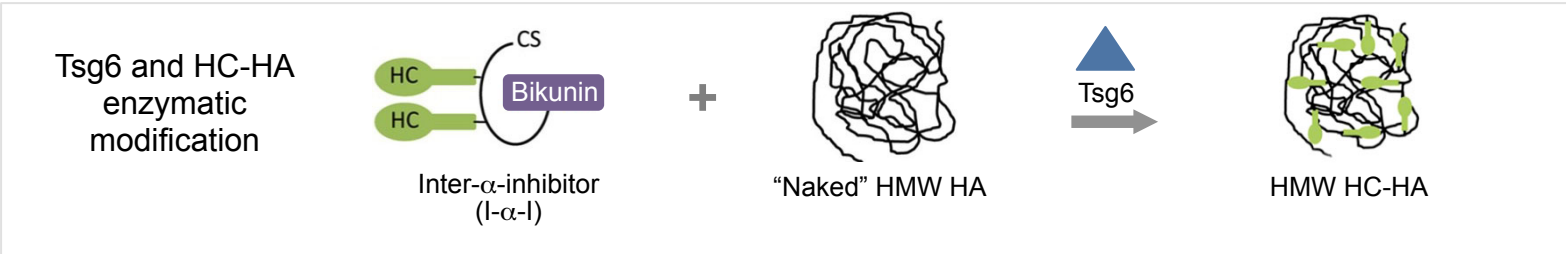

A *Tsg6* -/- mice may be predisposed to midgut volvulus (E18.5)

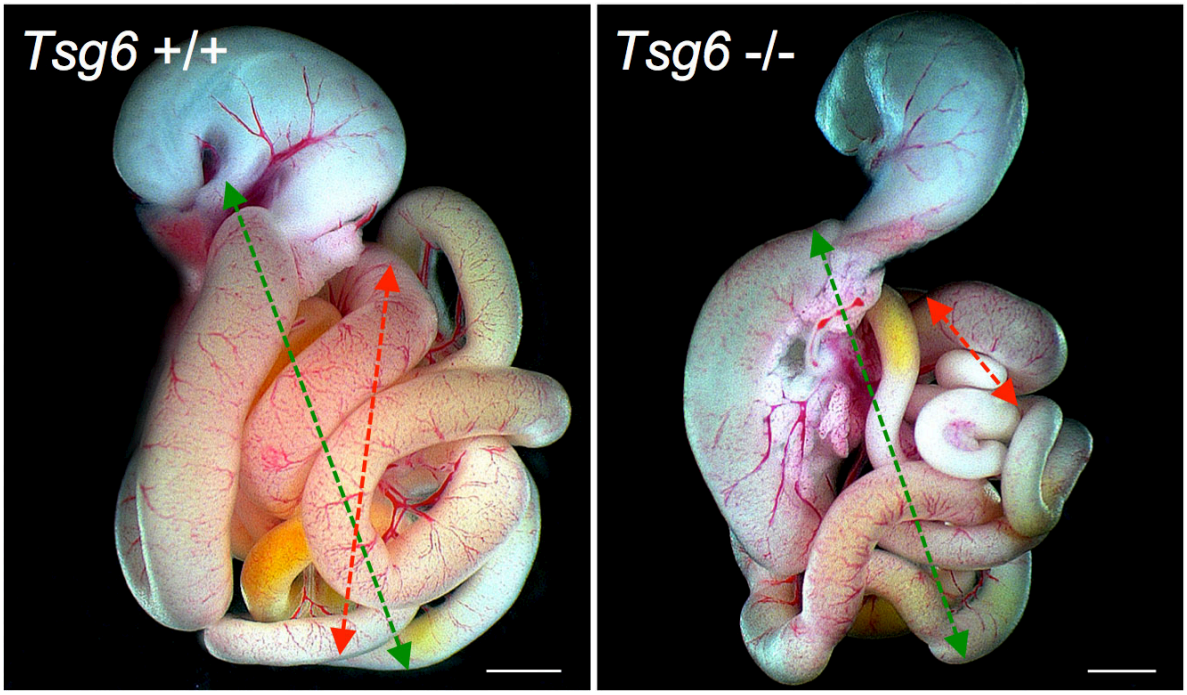

Green: abdominal length
Red: Distance between ICJ (top) and DJJ (bottom)

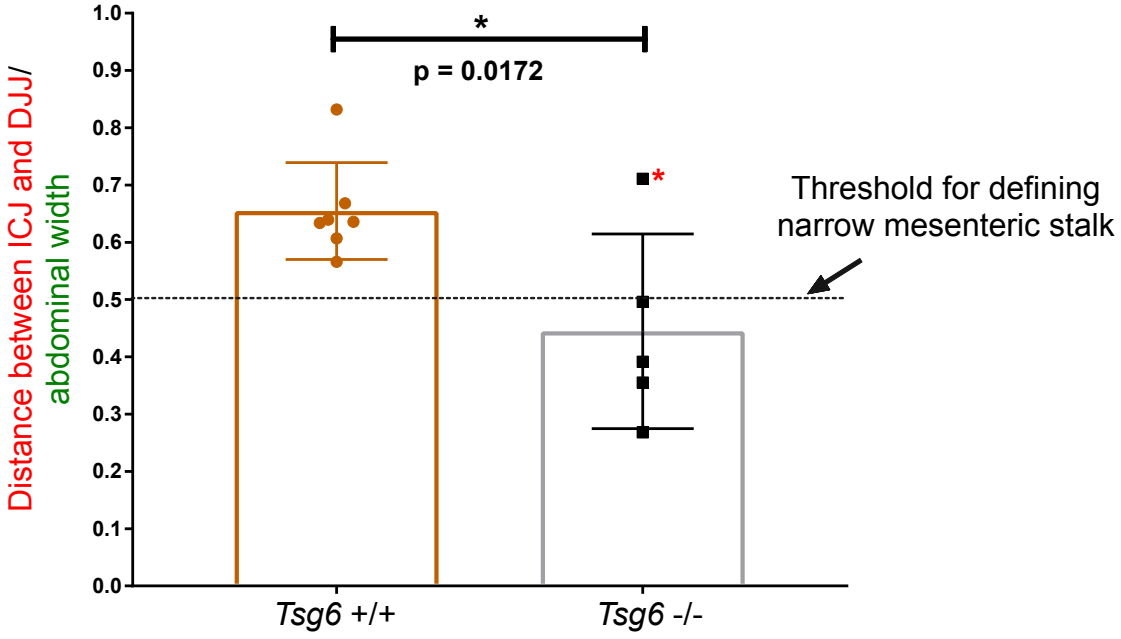

B *Tsg6* -/- mice display altered gut looping chirality (E13.5)

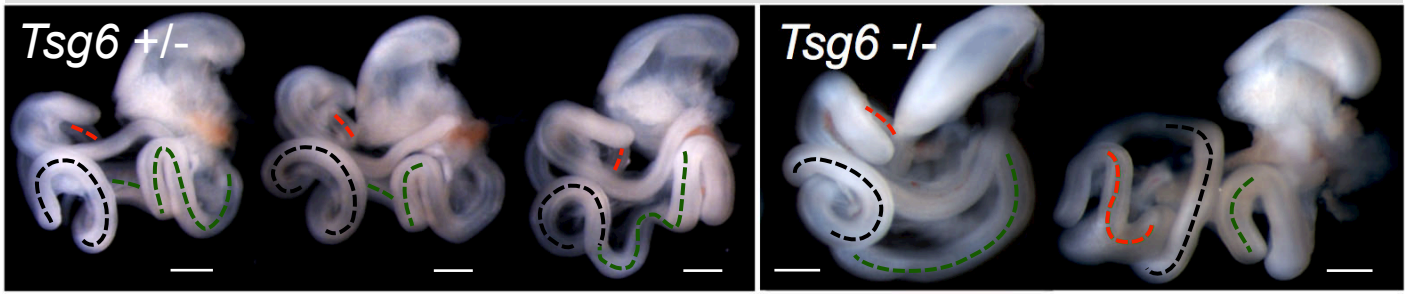

GENOTYPES OF TSG6 MOUSE EMBRYOS

Tsg6 cross		**Het x Het**					**Het x Mut**		
	Total Offspring		32					85	
Genotype		**+/+**	**:**	**+/-**	**:**	**-/-**	**+/-**	**:**	**-/-**
Counts	Expected	8	:	16	:	8	42.5	:	42.5
	Observed	**6**	**:**	**21**	**:**	**5**	**59**	**:**	**26 [30%]**
Ratios	Expected	1	:	2	:	1	1	:	1
	Observed	**1.2**	**:**	**4.2**	**:**	**1**	**2.26**	**:**	**1**